

# In-situ measurement of CO<sub>2</sub> at the Xinglong regional background station over North China

YANG Yang<sup>a,b</sup>, WANG Ting<sup>a</sup>, WANG Pucui<sup>a,b</sup>, ZHOU Minqiang<sup>c</sup> and YAO Bo<sup>d</sup>

<sup>a</sup>Key Laboratory of Middle Atmosphere and Global Environment Observation, Institute of Atmospheric Physics, Chinese Academy of Sciences, Beijing, China; <sup>b</sup>College of Earth and Planetary Science, University of Chinese Academy of Sciences, Beijing, China; <sup>c</sup>Royal Belgian Institute for Space Aeronomy, Brussels, Belgium; <sup>d</sup>Meteorological Observation Center of China Meteorological Administration, Beijing, China

## ABSTRACT

High-accuracy continuous measurements of atmospheric concentrations of CO<sub>2</sub> were made from May 2016 to December 2017 using the Picarro G2301 analyzer at Xinglong station (40°24'N, 117°30'E, 940 MSL), 150 km northeast of Beijing. The near-ground CO<sub>2</sub> measurements were calibrated by standards based on WMO procedures. The regional background measurements were filtered by the robust extraction of baseline signal method to study the seasonal and diurnal cycles. The regional background CO<sub>2</sub> concentrations were low in summer. The maximum difference between the local sources and regional background CO<sub>2</sub> concentrations occurred in summer and autumn, indicating a strong influence from local sources. Cluster analysis and potential source contribution function analysis showed that the long-distance transport of anthropogenic emissions in the Beijing–Tianjin–Hebei metropolitan area influenced the CO<sub>2</sub> concentrations in Xinglong, especially in summer. The diurnal variation of CO<sub>2</sub> was mainly influenced by the various vertical transport conditions of the tropospheric atmosphere in a day.

## ARTICLE HISTORY

Received 8 November 2018  
Revised 12 February 2019  
Accepted 9 April 2019

## KEYWORDS

Xinglong station; CO<sub>2</sub> concentration; variation; source analysis

## 关键词

兴隆站; CO<sub>2</sub>浓度; 变化趋势; 远距离输送

## 华北地区兴隆站二氧化碳浓度观测

### 摘要

基于兴隆站Picarro G2301观测资料, 本文分析了2016年5月至2017年12月近地面二氧化碳浓度变化趋势以及远距离输送的影响。采用背景值筛选方法, 提取了兴隆站二氧化碳背景浓度和污染浓度。分析表明, 兴隆站二氧化碳背景浓度和污染浓度有相似的季节变化特征, 夏季最低, 冬季和早春较高。冬季和早春的高背景值主要由于正的生物通量, 即更强的植物呼吸作用和更弱的植物光合作用; 夏季则相反, 夏季和初秋污染浓度与背景浓度差值均较大, 主要是本地源排放增加, 而72小时后向轨迹的聚类分析以及PSCF分析也表明, 夏季由于来自北京, 天津, 河北和山东的气流输送, 携带有高浓度二氧化碳气团也会使兴隆地区的二氧化碳污染浓度升高。远距离输送结果也表明, 京津冀区域人为排放二氧化碳对兴隆地区四个季节的二氧化碳浓度均有正的贡献, 冬季来自内蒙古和张家口的气团输送也会带来正的贡献。二氧化碳浓度的日变化在所有季节都很显著, 10:00至14:00左右二氧化碳浓度较低。中午较强的边界层对流将高空低浓度的二氧化碳向下输送到近地面大气, 下午则相反, 而高值通常发生在夜间。

## 1. Introduction

The continuous increases in the concentrations of greenhouse gases, particularly CO<sub>2</sub>, have attracted much attention from the international community. The global average concentration of atmospheric CO<sub>2</sub> has increased by 145% since the pre-industrial era and was up to 403.3 ± 0.1 ppm in 2016 (WMO 2017). CO<sub>2</sub> has a long lifetime in the atmosphere and contributes >60% of the total radiative forcing of greenhouse gases, although it accounts for a relatively small proportion of the total amount of gas in the atmosphere (IPCC 2013). The increase in atmospheric concentrations of CO<sub>2</sub> is mainly attributed to the burning of fossil

fuels and changes in land use (Peters et al. 2011). The sources and sinks of CO<sub>2</sub> in the atmosphere are unevenly distributed and subject to a variety of transport processes. High-precision measurements of the concentrations of CO<sub>2</sub> provide a foundation for the assessment of carbon emissions and studies of the carbon cycle (Andrews et al. 2014; Fang et al. 2014).

Governments and research groups have put much effort into monitoring and quantifying the magnitude and distribution of greenhouse gases at both domestic and international levels. To date, there are more than 150 sites worldwide in the World Meteorology Organization/Global Atmosphere Watch (WMO/GAW) network, with

CONTACT WANG Ting  wangting@mail.iap.ac.cn

 Supplemental data for this article can be [here](#).

© 2019 The Author(s). Published by Informa UK Limited, trading as Taylor & Francis Group.

This is an Open Access article distributed under the terms of the Creative Commons Attribution License (<http://creativecommons.org/licenses/by/4.0/>), which permits unrestricted use, distribution, and reproduction in any medium, provided the original work is properly cited.

the aim of detecting changes in greenhouse gas concentrations and source–sink analysis. The USA has conducted long-term observations of atmospheric CO<sub>2</sub> concentrations at the Mauna Loa site in Hawaii since 1958. The US National Oceanic and Atmospheric Administration (NOAA) Earth System Research Laboratory have been working to build a network of tall-tower CO<sub>2</sub> measurement sites since the early 1990s (Bakwin et al. 1998; Zhao, Bakwin, and Tans 1997) and a reliable and precise in-situ CO<sub>2</sub> analysis system has been developed and deployed at eight sites in the NOAA Earth System Research Laboratory Global Greenhouse Gas Reference Network. The Integrated Carbon Observation System in Europe is committed to providing high-precision data to determine the spatial distributions of long-term changes in CO<sub>2</sub> concentrations (Yver Kwok et al. 2015).

The concentrations of greenhouse gases in China are increasing quickly due to rapid economic growth and the increased combustion of fossil fuels. Since the 1990s, seven CO<sub>2</sub>/CH<sub>4</sub> background stations have been set up by the China Meteorological Administration (CMA), and four of them — Waliguan in Qinghai Province, Shangdianzi in Beijing, Lin'an in Zhejiang Province, and Longfeng Mountain in Heilongjiang Province (Fang et al. 2014; Liu et al. 2009) — belong to the WMO/GAW global network.

Measurements of CO<sub>2</sub> in economically developed and densely populated areas of China are important due to the impact of human activities, especially in the Beijing–Tianjin–Hebei metropolitan area. Xinglong station is located in Xinglong County, Hebei Province, and can be used as a background station for the Beijing–Tianjin–Hebei metropolitan area (Cheng et al. 2003). A Picarro cavity ring-down spectroscopy (CRDS) analyzer is used for monitoring carbon emissions.

## 2. Data and methods

### 2.1. In-situ measurement methods

Xinglong station (40°24'N, 117°30'E, 940 MSL) (red spot in Figure S1) is located in Xinglong County, Hebei Province, south of the Yanshan Mountains, about 150 km northeast of Beijing. It is surrounded by mountains with shrubland and grassland. Also, there are no industrial activities within 20 km. Xinglong station is far from megacities and major transport routes and the atmospheric conditions may, therefore, represent the regional atmosphere (Wu et al. 2010).

Based on CRDS techniques, the Picarro instrument is designed as a low drift, high-precision greenhouse gas analyzer. The intensity of the laser introduced into a high-precision optical cavity decays exponentially with time.

The decay time constant,  $\tau$ , depends on the loss during the transport between different endoscopes in the optical cavity and the absorption and scattering of the sample being measured. The concentration of the gas sample is related to  $\tau$  (Crosson 2008). CO<sub>2</sub> concentrations have been observed at Xinglong station using the Picarro G2301 high-precision CRDS analyzer since May 2016. The instrument sampling inlet is located on the roof of a three-story building and has been operated for more than 1 year.

### 2.2. Data processing

#### 2.2.1. Calibration

Eight calibrations were performed from 14 November to 14 December 2017, with a duration of 15 min for each calibration, to determine the stability of the G2301 high-precision CRDS analyzer. Standard gas, with a CH<sub>4</sub> concentration of  $2036.5 \pm 0.3$  ppb and a CO<sub>2</sub> concentration of  $399.95 \pm 0.02$  ppm under dry and clean atmospheric conditions was calibrated by the Meteorological Observation Center of the CMA based on the WMO X2007 scale for CO<sub>2</sub>.

The response of the analyzer is unstable after the start of calibration as a result of the time required for flushing the internal volume of the analyzer (Yan et al. 2011). We set the flushing time to 5 min and therefore only data obtained 5 min after the start of the calibration were retained. The temporal resolution of the raw data was 5 s, but 1-min average values were used for the calibration analysis and 1-h average values elsewhere.

#### 2.2.2. Data filtering

The robust extraction of baseline signal method (Thoning, Tans, and Komhyr 1989; Fang et al. 2015) is always used to classify the regional background and non-background CO<sub>2</sub> measurements. The regional background measurements showed that the air was well mixed and not affected by local anthropogenic emissions and regional transport. The concentrations higher than the regional background values were governed by regional or local sources, usually reflecting significant changes in concentration over short periods of time — for example, the rapid increase in concentrations during daytime due to human activities (Zhang, Zhou, and Xu 2013). Concentrations lower than the regional background values represent local sinks.

The data were filtered with a method similar to that of Ruckstuhl et al. (2012): (1) all the outliers introduced by system failure or other factors were flagged; (2) the 30-day running average and standard deviation  $\sigma$  of the measurements were calculated; and (3) the absolute difference between each measurement and the running average was calculated. The measurements were flagged

and considered as non-background data if this difference exceeded  $\sigma$ . The final extracted data were considered to represent the fluctuations in regional background CO<sub>2</sub> concentrations at Xinglong station. The remaining measurements were either sources or sinks, tagged, respectively, by values higher or lower than that of the regional background (Zhang, Zhou, and Xu 2013).

The total number of hourly mean CO<sub>2</sub> samples was 13 077 during the observation period, including 9680 regional background measurements (74.0%).

### 3. Results and discussion

#### 3.1. Instrument stability

The upper panels in Figure S2 show the differences (Andrews et al. 2014) between the CO<sub>2</sub> concentrations in atmosphere and calibration tanks. The average differences for CO<sub>2</sub> are stable around  $\pm 0.1$  ppm during the calibration period, confirming that the accuracies of our measurements meet the WMO/GAW criteria of  $\pm 0.1$  ppm for CO<sub>2</sub> (Tuomas 2007).

As the differences in the values for CO<sub>2</sub> were small relative to their concentrations, we considered the calibration coefficients during each calibration to be the ratio of the measured value and the standard value, as shown in the lower panel. The calibration coefficients for CO<sub>2</sub> were stable at 0.992–0.993. We used the average calibration coefficients for CO<sub>2</sub> to calibrate the raw data.

#### 3.2. Seasonal and diurnal variations

Figure 1 shows the time series of CO<sub>2</sub> concentrations in Xinglong during the period June 2016 to December 2017. The black dots are the filtered regional background values based on the robust extraction of the baseline signal.

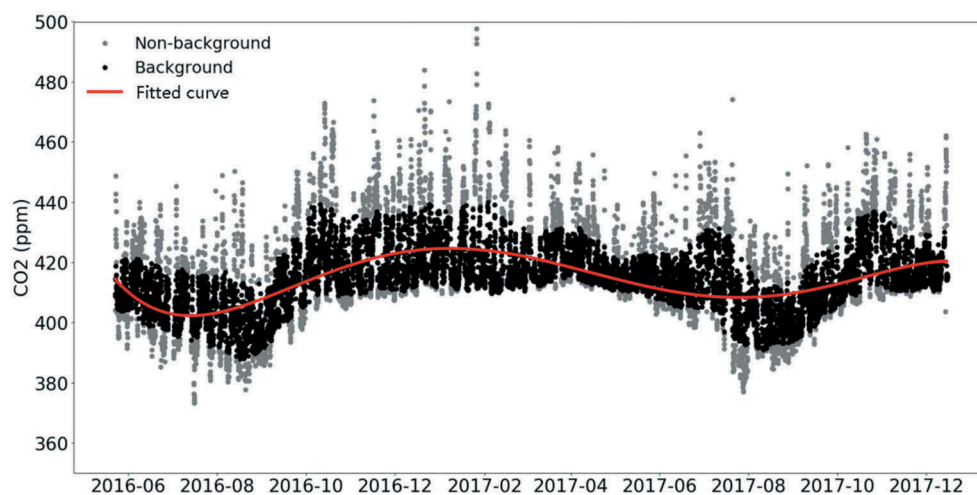


Figure 1. Time series of regional background (black) and non-background (gray) CO<sub>2</sub> concentrations in Xinglong.

Figure 2 shows the monthly cycles of local sources and regional background CO<sub>2</sub> concentrations over a 12-month period and the upper panel shows their differences. Figure 2 shows that both the local sources and regional background CO<sub>2</sub> concentrations are low in summer, the season with the strongest photosynthetic uptake. The high regional background values in winter and early spring are due to positive biological fluxes (i.e., stronger plant respiration and weaker plant photosynthesis). The seasonal variations in Shangdianzi, which is also located in the Beijing–Tianjin–Hebei urban agglomeration on the North China Plain, are almost identical compared to that in Xinglong, with the lowest occurring in August and highest in March (Xia et al. 2016). In addition to weaker plant photosynthesis, CO<sub>2</sub> occupies 6.13% of the total emissions

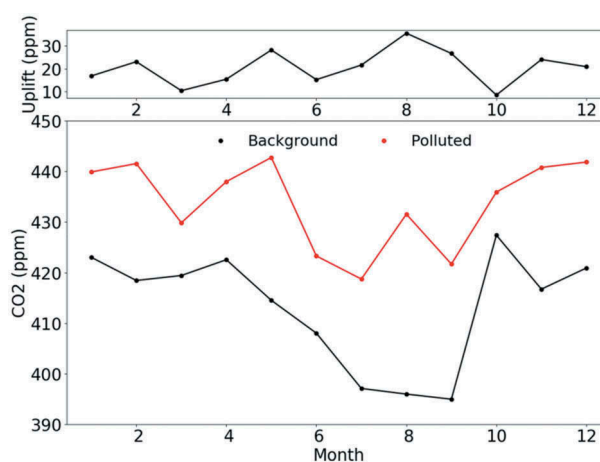


Figure 2. Monthly cycles of local sources and regional background CO<sub>2</sub> concentrations over a 12-month period. The upper panel shows the differences between the local sources and regional background CO<sub>2</sub> concentrations over a 12-month period. The lower panel shows the monthly cycles of local sources and regional background CO<sub>2</sub> concentrations over a 12-month period.

from straw burning in China in autumn (Cao et al. 2008), influencing the regional background signal in Xinglong in October. The increase in anthropogenic sources of CO<sub>2</sub> from domestic heating contributes to the higher CO<sub>2</sub> values during winter (Wang et al. 2010). The peak-to-trough value of the monthly regional background CO<sub>2</sub> concentration is  $32.43 \pm 10.95$  ppm, proving the obvious seasonal variation in CO<sub>2</sub> in Xinglong station. Differences in the local sources and regional background CO<sub>2</sub> concentrations (upper panel in Figure 2) are large in summer and early autumn, reaching  $21.63 \pm 7.40$ ,  $35.56 \pm 7.40$ , and  $26.72 \pm 7.40$  ppm in July, August, and September, respectively (Fang et al. 2017). This indicates the strong influence of strong local sources in these two seasons. The relatively higher discrepancies in November and February also illustrate higher signals from local sources.

The least-squares method was used to fit the hourly average data of CO<sub>2</sub> to evaluate the diurnal cycles in the regional background CO<sub>2</sub> concentrations in different seasons that were not affected by linear trends. Figure 3 shows four diurnal cycles of CO<sub>2</sub>.

In general, the diurnal variations in CO<sub>2</sub> concentrations are significant in all seasons, with low values around 1000 to 1400 local time. This is because the stronger convection at noon mixes the near-ground high CO<sub>2</sub> concentrations with the low concentrations in the upper-level atmosphere. The weaker convective diffusion in the boundary layer limits the accumulation of CO<sub>2</sub> in the afternoon and high values usually occur at night. The peak-to-trough diurnal amplitudes are  $2.82 \pm 0.93$ ,  $3.97 \pm 1.26$ ,  $3.58 \pm 1.26$ , and  $4.10 \pm 1.06$  ppm for spring, summer, autumn, and winter, respectively.

### 3.3. Influence of long-distance transport

Xinglong station is built on a relatively high hill and CO<sub>2</sub> concentrations are likely due to large-scale advection (Fang et al. 2016). We calculated the backward 72-h

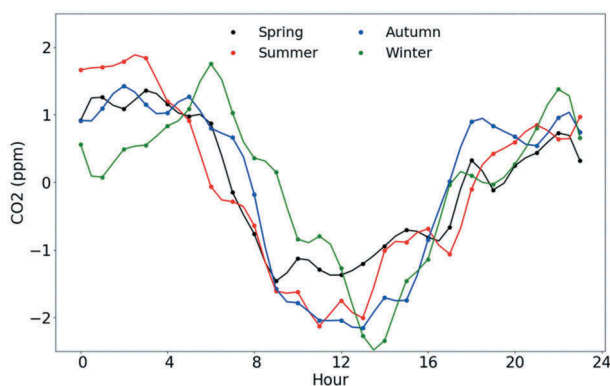


**Figure 3.** Diurnal cycles of regional background concentrations of CO<sub>2</sub> by season.

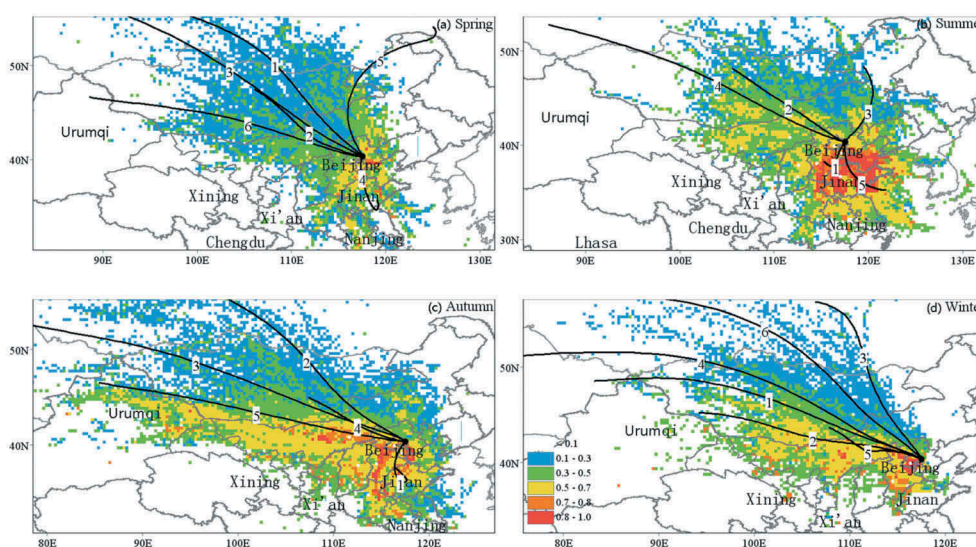
airflow trajectories arriving in the Xinglong area in all four seasons from May 2016 to December 2017 based on Meteoinfo software to analyze the long-distance transport contributing to CO<sub>2</sub> concentrations. Cluster analysis groups a large number of trajectories according to the horizontal movement velocity as well as the direction of the air masses and is applied to the analysis of the classification of different transportation (Shi et al. 2008). Based on the potential source contribution function (PSCF) algorithm, we calculated the quantitative contributions of potential areas for CO<sub>2</sub> in all four seasons in Xinglong (Begum et al. 2005).

Figure 4 shows the patterns of cluster analysis for the major 72-h backward trajectories in each season and the potential source contribution of CO<sub>2</sub> in Xinglong from May 2016 to December 2017. The numbers indicate the trajectory clustering type. The PSCF analysis is also shown in Figure 4 as a supplement to the backward trajectory analysis. The shading represents the probability distribution of emission sources. Table 1 shows the cluster analysis of trajectories, the average CO<sub>2</sub> concentrations in each cluster, and the regions the clusters run through.

Most of the clusters in spring have pathways northwest of the station, where Mongolia, Russia and Zhangjiakou (in Hebei Province) are located. However, these regions are not expected to be a major contributor for clusters 1, 2, 3, and 6 (covering about 74.32%), which have lower mean CO<sub>2</sub> concentrations. Cluster 4 may transport anthropogenic emissions with relatively high CO<sub>2</sub> concentrations of  $418.68 \pm 10.95$  ppm, from Tangshan and Tianjin. The slower speed of cluster 4 obstructs the dilution of strong emissions and hence CO<sub>2</sub> is accumulated before arriving in Xinglong.

The CO<sub>2</sub> concentrations in summer are more influenced by clusters 1 and 5 with higher CO<sub>2</sub> concentrations running through Beijing–Tianjin–Hebei and Shandong. Clusters 1 and 5 account for about 47.79%. Clusters 2 and 4, from Mongolia and Zhangjiakou, together with cluster 3 from the east of Inner Mongolia and Chifeng, are considered as relatively clean areas with lower CO<sub>2</sub> concentrations.

In autumn and winter, with the strong invasion of westerly wind, the west–north–west clusters through Mongolia, Urumqi, and Zhangjiakou all transport large amounts of CO<sub>2</sub>. The urban agglomerations of Beijing–Tianjin–Hebei and Shandong also make a positive contribution to the concentrations of CO<sub>2</sub> in Xinglong in autumn, with the highest values of  $418.11 \pm 13.20$  ppm for CO<sub>2</sub> carried by cluster 1. Although there is no obvious airflow from the Beijing–Tianjin–Hebei metropolitan area, the PSCF analysis shows that the anthropogenic emissions from these areas also make a large contribution to CO<sub>2</sub> concentrations in winter. Liu et al. (2009) also studied the



**Figure 4.** Cluster analysis of 72-h backward trajectory and PSCF analysis of CO<sub>2</sub> in Xinglong from May 2016 to December 2017. The numbers indicate the trajectory clustering type and the color depth represents the probability distribution of the emission sources: the deeper the color, the greater the contribution.

**Table 1.** Statistical analysis of cluster trajectories, including trajectory numbers, ratios, average CO<sub>2</sub> concentrations in each cluster, and the regions each cluster runs through.

Season	Cluster	Trajectory number	Ratio	Average CO <sub>2</sub> (ppm)	Through-regions
Spring	4	425	16.00%	418.68 ± 10.95	Tangshan and Tianjin in China
	2	714	26.88%	414.68 ± 8.49	Mongolia and Russia, Zhangjiakou in China
	6	436	16.42%	416.69 ± 9.18	
	3	318	11.97%	411.18 ± 7.48	
	1	506	19.05%	411.07 ± 5.65	
	5	257	9.68%	413.26 ± 3.14	Mongolia, north of the station
Summer	1	1133	28.53%	407.30 ± 12.79	Beijing–Tianjin–Hebei and Shandong in China
	5	765	19.26%	409.85 ± 10.99	
	4	322	8.11%	404.81 ± 14.05	Mongolia, Zhangjiakou in China
	2	1058	26.64%	401.43 ± 12.16	
Autumn	3	693	17.45%	397.41 ± 11.03	Inner Mongolia and Chifeng in China
	1	680	17.33%	418.11 ± 13.20	Beijing–Tianjin–Hebei and Shandong in China
	3	686	17.48%	416.99 ± 12.52	Mongolia, Zhangjiakou and Wulumuqi in China
	4	1110	28.29%	417.05 ± 13.66	
	5	844	21.51%	417.94 ± 13.49	
Winter	2	604	15.39%	408.38 ± 8.79	Mongolia
	4	171	6.56%	423.84 ± 16.60	Mongolia and Russia, Zhangjiakou in Hebei
	2	516	19.79%	426.49 ± 12.99	
	5	485	18.60%	425.26 ± 13.64	
	1	526	20.17%	420.39 ± 12.28	
	6	394	15.11%	412.54 ± 6.21	Mongolia
	3	516	19.79%	413.17 ± 5.61	

relationship between the winds and the non-background CO<sub>2</sub> in Shangdianzi. They concluded that transport from Beijing–Tianjin–Hebei makes apparently positive contributions to the non-background CO<sub>2</sub> in Shangdianzi station, which acts similar to Xinglong station.

The PSCF (shaded areas in Figure 4) was also studied in addition to the cluster analysis of the 72-h backward trajectory. In spring, in addition to the regions determined from the cluster analysis, there is also a possible contribution from the cities in eastern Hebei Province. In summer, the potential sources of CO<sub>2</sub> are restricted to the south of the station, mainly in Hebei Province.

The potential contributing areas in autumn for CO<sub>2</sub> are mainly located in two main directions: south to Henan Province and west-northwest to Inner Mongolia. Potential source areas for CO<sub>2</sub> in winter are concentrated in Beijing, north of Shanxi Province and west-northwest to Inner Mongolia.

#### 4. Conclusions

This paper reports continuous measurements of atmospheric CO<sub>2</sub> in Xinglong from May 2016 to December 2017. The seasonal and diurnal variations in

CO<sub>2</sub> concentrations, together with long-distance transport, are discussed.

The accuracy of the Picarro instrument in Xinglong meets the requirements of the WMO/GAW global network. The CO<sub>2</sub> concentrations are high in winter and low in summer. The seasonal variation in the regional background concentrations of CO<sub>2</sub> is mainly due to the photosynthesis and respiration of plants. Regional transport is another important factor. The air mass from southwest, south, and southeast of the station (e.g., from Beijing, Hebei Province, and Shandong Province) contributes to the high CO<sub>2</sub> concentrations, especially in summer. Transport from Inner Mongolia is another potential source for CO<sub>2</sub> in autumn and winter.

The diurnal patterns in CO<sub>2</sub> concentrations show relatively low values around 1000–1400 local time. For CO<sub>2</sub>, the strong sunshine at noon results in stronger mixing of the near-surface atmosphere with that at higher levels, which dilutes the near-ground CO<sub>2</sub> concentrations. The more stable and lower boundary layer in the afternoon increases the concentrations of CO<sub>2</sub>.

The measurements at Xinglong are made continuously and with regular calibration. With more collected data, we will be capable of analyzing the changes/trends of CO<sub>2</sub> in the near future. Meanwhile, instead of the regional background CO<sub>2</sub> measurements, we intend to study the relatively high and low CO<sub>2</sub> measurements and try to better understand the sources and sinks of CO<sub>2</sub> around Xinglong.

## Acknowledgments

We express our great thanks to the staff at Xinglong station who contributed to the instrument's maintenance at the station.

## Disclosure statement

No potential conflict of interest was reported by the authors.

## Funding

This research was funded by the National Key Research and Development Program of China [grant numbers 2017YFB0504000 and 2017YFC1501701] and the National Natural Science Foundation of China [grant number 41575034].

## References

- Andrews, A. E., J. D. Kofler, M. E. Trudeau, J. C. Williams, D. H. Neff, K. A. Masarie, D. Y. Chao, et al. 2014. "CO<sub>2</sub>, CO, and CH<sub>4</sub> Measurements from Tall Towers in the NOAA Earth System Research Laboratory's Global Greenhouse Gas Reference Network: Instrumentation, Uncertainty Analysis, and Recommendations for Future High-accuracy Greenhouse Gas Monitoring Efforts." *Atmos. Meas. Tech.*, 7: 647–687. doi:10.5194/amt-7-647-2014.
- Bakwin, P. S., P. P. Tans, D. F. Hurst, and C. L. Zhao. 1998. "Measurements of Carbon Dioxide on Very Tall Towers: Results of the NOAA/CMDL Program." *Tellus* 50 (B): 401–415. doi:10.3402/tellusb.v50i5.16216.
- Begum, B. A., E. Kim, C. H. Jeong, D.-W. Lee, and P.K. Hopke. 2005. "Evaluation of the Potential Source Contribution Function Using the 2002 Quebec Forest Fire Episode." *Atmospheric Environment* 39: 3719–3724. doi:10.1016/j.atmosenv.2005.03.008.
- Cao, G. L., X. Y. Zhang, Y. Q. Wang, and F. C. Zheng. 2008. "Estimation of Emissions from Field Burning of Crop Straw in China." *Chinese Science Bulletin* 53 (5): 784–790. doi:10.1007/s11434-008-0145-4.
- Cheng, H. B., M. L. Wang, Y. X. Wen, and G. C. Wang. 2003. "Background Concentrations of Greenhouse Gases CO<sub>2</sub>, CH<sub>4</sub>, and N<sub>2</sub>O at Mt.waliguan and Xinglong Stations in China." *Journal of Applied Meteorology* 14 (4): 402–409.
- Crosson, E. R. 2008. "A Cavity Ring-down Analyzer for Measuring Atmospheric Levels of Methane, Carbon Dioxide, and Water Vapor." *Applied Physics B* 92 (3): 403–408. doi:10.1007/s00340-008-3135-y.
- Fang, S. X., L. X. Zhou, P. P. Tans, P. Ciais, M. Steinbacher, L. Xu, and T. Luan. 2014. "In Situ Measurement of Atmospheric CO<sub>2</sub> at the Four WMO/GAW Stations in China." *Atmospheric Chemistry and Physics* 14: 2541–2554. doi:10.5194/acp-14-2541-2014.
- Fang, S. X., P. P. Tans, B. Yao, T. Luan, Y. L. Wu, and D. J. Yu. 2017. "Study of Atmospheric CO<sub>2</sub> and CH<sub>4</sub> at Longfengshan WMO/GAW Regional Station: The Variations, Trends, Influence of Local Sources/sinks, and Transport." *Science China Earth Sciences* 60: 1886–1895. doi:10.1007/s11430-016-9066-3.
- Fang, S. X., P. P. Tans, M. Steinbacher, L. X. Zhou, T. Luan, and Z. Li. 2016. "Observation of Atmospheric CO<sub>2</sub> and CO at Shangri-La Station: Results from the Only Regional Station Located at Southwestern China." *Tellus B: Chemical and Physical Meteorology* 68: 1–13. doi:10.3402/tellusb.v68.28506.
- Fang, S. X., T. Luan, G. Zhang, Y. L. Wu, and D. J. Yu. 2015. "The Determination of Regional CO<sub>2</sub> Mole Fractions at the Longfengshan WMO/GAW Station: A Comparison of Four Data Filtering Approaches." *Atmospheric Environment* 116 (10): 36–43. doi:10.1016/j.atmosenv.2015.05.059.
- IPCC-Intergovernmental Panel on Climate Change: Climate Change. 2013. *The Physical Science Basis, Fifth Assessment Report of the Intergovernmental Panel on Climate Change*. New York: Cambridge University Press.
- Liu, L. X., L. X. Zhou, X. C. Zhang, M. Wen, F. Zhang, B. Yao, and S. X. Fang. 2009. "Characteristics of Atmospheric CO<sub>2</sub> Background Changes at Four National Level Stations in China." *Science China Earth Sciences* 39: 222–228. doi:10.1007/s11430-009-0143-7.
- Peters, G. P., G. Marland, C. Le Quééré, T. Boden, J. G. Canadell, and M. R. Raupach. 2011. "Rapid Growth in CO<sub>2</sub> Emissions after the 2008–2009 Global Financial Crisis." *Nature Climate Change* 2: 2–4. doi:10.1038/nclimate1332.
- Ruckstuhl, A. F., S. Henne, S. Reimann, M. Steinbacher, M. K. Vollmer, S. O'Doherty, B. Buchmann, and C. Hueglin. 2012. "Robust Extraction of Baseline Signal of Atmospheric Trace Species Using Local Regression." *Atmospheric Measurement Techniques* 5: 2613–2624. doi:10.5194/amt-5-2613-2012.

- Shi, C. E., Y. Q. Yao, P. Zhang, and M. Y. Qiu. 2008. "Transport Trajectory Classifying Of Pm10 in Hefei." *Plateau Meteorology (In Chinese)* 6: 330–341.
- Thoning, K. W., P. P. Tans, and W. D. Komhyr. 1989. "Atmospheric Carbon Dioxide at Mauna Loa Observatory 2. Analysis of the NOAA GMCC Data, 1974–1985." *Journal of Geophysical Research Atmospheres* 94 (D6): 8549–8565. doi:10.1029/JD094iD06p08549.
- Tuomas, L. 2007. "World Meteorological Organization Global Atmosphere Watch." *World Meteorological Organization*, 145.
- Wang, Y., J. W. Munger, S. Xu, M. B. McElroy, J. Hao, C. P. Nielsen, and H. Ma. 2010. "CO<sub>2</sub> and Its Correlation with CO at a Rural Site near Beijing: Implications for Combustion Efficiency in China." *Atmospheric Measurement Techniques* 10: 8881–8897. doi:10.5194/acp-10-8881-2010.
- WMO data summary. 2017. "WMO World Data Centre for Greenhouse Gases (WDCGG) Data Summary: Greenhouse Gases and Other Atmospheric Gases, No. 41." *Japan Meteorological Agency*. <http://ds.data.jma.go.jp/gmd/wdcgg/pub/products/summary/sum41/sum41.pdf>
- Wu, D., J. Y. Xin, Y. Sun, Y. S. Wang, and P. C. Wang. 2010. "Variation and Analysis of Background Concentration of Atmospheric Pollutants in North China during the 2008 Olympic Games." *Environmental Science* 31 (5): 1130–1138.
- Xia, L. J., L. X. Zhou, L. X. Liu, and G. Zhang. 2016. "monitoring Atmospheric CO<sub>2</sub> and δ<sup>13</sup>C(CO<sub>2</sub>) Background Levels at Shangdianzi Station in Beijing, China." *Environmental Science (In Chinese)*. 30: 2.
- Yan, K. P., L. X. Zhou, S. X. Fang, Y. X. Wen, B. Yao, F. Zhang, and L. X. Liu. 2011. "Flow and Method of Calibration Based on the New CO<sub>2</sub> and CH<sub>4</sub> Mixed Standard Gases." *Environmental Chemistry* 37 (4): 511–516.
- Yver Kwok, C., O. Laurent, A. Guemri, C. Philippon, B. Wastine, C. W. Rella, C. Vuillemin, et al. 2015. "Comprehensive Laboratory and Field Testing of Cavity Ring-down Spectroscopy Analyzers Measuring H<sub>2</sub>O, CO<sub>2</sub>, CH<sub>4</sub> and CO." *Atmospheric Measurement Techniques* 8: 3867–3892. doi:10.5194/amt-8-3867-2015.
- Zhang, F., L. M. Zhou, and L. Xu. 2013. "Analysis of Variation of CH<sub>4</sub> Concentration in the Atmosphere of Waliguan and Its Potential Source Regions." *Science China: Earth Sciences* 56: 727–736. doi:10.1007/s11430-012-4577-y.
- Zhao, C. L., P. S. Bakwin, and P. P. Tans. 1997. "A Design for Unattended Monitoring of Carbon Dioxide on A Very Tall Tower." *Atmospheric and Oceanic Science Letters* 14: 1139–1145. doi:10.1175/1520-0426(1997)014<1139:ADFUMO>2.0.CO;2.